Research article Available online www.ijsrr.org ISSN: 2279–0543

International Journal of Scientific Research and Reviews

Nanofluid Flow in an Inclined Artery With Overlapping Stenosis and Permeable Walls

Kawkab Tahmeena [1*], Kumar Y.V. K. Ravi [2] and Devi C. Uma[3]

[1*] Dept. of Mathematics, Rayala Seema University, Kurnool, A.P, India.
Email : tahmeenakawkab1@gmail.com
[2]Dept. of Mathematics, BITS Pilani, Hyderabad Center, Hyderbad, Telangana, India.
Email : yvkravikumar@pilani.bits-pilani.ac.in
[3]Dept. of Mathematics, TKR CET, Hyderbad, Telangana, India.
Email : uma140276@gmail.com

ABSTRACT

In this paper, a mathematical model for nanofluid flow in an inclined artery with overlapping stenosis and permeable walls is presented. The analytical solutions are obtained for velocity, pressure drop, impedance and wall shear stress by taking mild stenosis into consideration. The effects of various parameters like height of stenosis, Brownian motion number, local nanoparticle Grashof number, local temperature Grashof number, inclination, thermophoresis parameter, Darcy number and slip parameter on velocity, temperature profile, nanoparticle phenomena, impedance, shear stress are analyzed. The behavior of blood is studied through the streamline patterns.

KEYWORDS: Nano fluid, blood flow, permeable walls, overlapping stenosis, Homotopy perturbation method**.**

***Corresponding Author**

Tahmeena Kawkab

Research Scholar,

Dept. of Mathematics,

Rayala Seema University, Kurnool, A.P, India.

E. Mail : tahmeenakawkab1@gmail.com

Mobile : +91-99 125 400 35

INTRODUCTION

In the recent times cardiovascular diseases have been one of the most severe diseases causing a large number of deaths in developed and developing countries. Most of these diseases are related to the abnormal flow of blood in stenotic arteries. Stenosis may result from embryonic mal development, hypertrophy and thickening of a sphincter muscle, inflammatory disorders or excessive development of fibrous tissue. It may involve almost any tube or duct. The development of stenosis in an artery can have serious consequences and can disturb the normal functioning of the circulatory system. In particular, it may lead to (i) increased resistance to flow, with possible severe reduction in blood flow (ii) increased danger of complete obstruction (iii) abnormal cellular growth in the vicinity of the stenosis, which increases the intensity of the stenosis, (iv) tissue damage leading to post stenotic dilatation. Hence detailed knowledge of the blood flow in stenosed arteries is required to understand and prevention of arterial diseases.

A number of theoretical and experimental investigations have been carried out to know the dynamics of blood flow through arteries with obstructions. These are categorized broadly according to the geometry of the arterial wall and blood rheology. The most common models which are developed to stimulate the arterial segments are the rigid tubes containing a single symmetric or non-symmetric stenosis [1-5]. However, stenosis may develop in series and may not be regular in shape or may be overlapping [6-9].

Nanofluids are a new class of fluids consisting of nano-sized particles(1 nm-100nm). Recently, the study of nanofluids has attracted many researchers because of its enormous applications in bio and mechanical industries such as heat transfer in microelectronics, fuel cells, and pharmaceutical processes etc. Nanofluids is the term which was first introduced by Choi[10] to describe new class of nanotechnology based heat transfer fluids with augmented thermal properties. The aim of nanofluids is to achieve the highest possible thermal properties at the smallest possible concentration by uniform dispersion and stable suspension of nanoparticles. Recent articles on nanofluids have been cited [11-13].

In the above mentioned research the walls of the tube are considered as rigid, but in physiological system the walls of the tube may be elastic, movable or permeable. Akbar et al.[14] had a theoretical investigation of nanofluid flow in a tapered stenosed artery with permeable walls. The effects of magnetic field for copper nanoparticles for blood flow through composite stenosis with permeable walls have been studied by Akbar and Wahid Butt [15]. Ellahi et al. [16] examined the blood flow of nanofluid through an artery with composite stenosis and permeable walls. In some physiological systems, the arteries may not be horizontal, but may be inclined with the axis. Maruthi Prasad et al.[17] studied the nanofluid flow in an inclined non-uniform tube with multiple constrictions.

Inspired by the above mentioned research, the aim of the present paper is to investigate the nanofluid flow of blood in an inclined tube with an overlapping stenosis and permeable walls. The non-linear coupled equations are solved by HPM. The solutions for velocity, temperature, pressure drop, resistance to the flow and wall shear stress are obtained by taking mild stenosis into consideration. The physical features of the major parameters are illustrated by graphs.

MATHEMATICAL FORMUALTION

Consider the steady, incompressible nanofluid flow in an inclined tube having overlapping stenosis with permeable walls makes an angle ' α ' to the z - axis [Fig. 1]. Cylindrical polar coordinate system (r, θ, z) is taken. Here z - axis coincides with the centre axis of the tube.

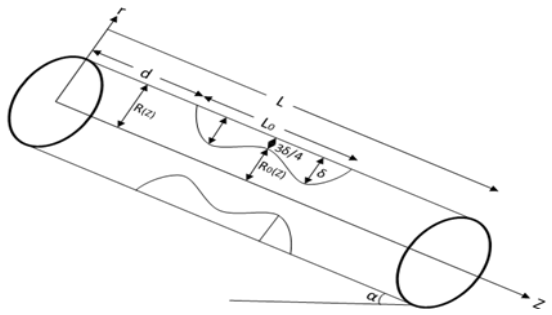

Figure 1: Geometry of an inclined tube with overlapping stenosis.

The geometry of the arterial wall of the overlapping stenosis is written mathematically as

$$h = \frac{R(z)}{Ro(z)}$$

$$= 1 - \frac{3}{2\left(\frac{\delta}{RoLo^4}[11(z-d)Lo^3 - 47(z-d)^2Lo^2 + 72(z-d)^3Lo - 36(z-d)^4]\right)}, \quad d \le z \le d + Lo,$$

$$= 1, \text{Otherwise.} \tag{1}$$

Where $R(Z)$ is the radius of the artery in the constricted region, $R_0(z)$ is the radius of the tube in the non-constricted region, L is the length of the tube, L_0 is the length of the stenosis and d shows the location of stenosis, δ the maximum height of the stenosis is shown at two locations $Z = d + \frac{L_0}{6}$, $Z = d + 5\frac{L_0}{6}$ respectively. The critical height of the stenosis $\frac{3\delta}{4}$ is located at $Z = d + \frac{L_0}{2}$, from the origin. The governing equations for the steady flow of an incompressible nanofluid are

$$\frac{1}{r}\frac{\partial(rv)}{\partial r} + \frac{\partial u}{\partial z} = 0, \tag{2}$$

$$\rho\left[v\frac{\partial v}{\partial r}+u\frac{\partial v}{\partial z}\right]=-\frac{\partial p}{\partial r}+\mu\left[\frac{\partial^2 v}{\partial r^2}+\frac{1}{r}\frac{\partial v}{\partial r}+\frac{\partial^2 v}{\partial z^2}-\frac{v}{r^2}\right]-\frac{\cos\alpha}{F}, \tag{3}$$

$$\rho\left[v\frac{\partial u}{\partial r}+u\frac{\partial u}{\partial z}\right]==-\frac{\partial p}{\partial z}+\mu\left[\frac{\partial^2 u}{\partial r^2}+\frac{1}{r}\frac{\partial u}{\partial r}+\frac{\partial^2 u}{\partial z^2}\right]+\rho g\alpha(T-T_0)+\rho g\alpha(C-C_0)+\frac{\sin\alpha}{F}, \tag{4}$$

$$\left[v\frac{\partial T}{\partial r}+u\frac{\partial T}{\partial z}\right]=\alpha\left[\frac{\partial^2 T}{\partial r^2}+\frac{1}{r}\frac{\partial T}{\partial r}+\frac{\partial^2 T}{\partial z^2}\right]+\tau\left\{D_B\left[\frac{\partial C}{\partial r}\frac{\partial T}{\partial r}+\frac{\partial C}{\partial z}\frac{\partial T}{\partial z}\right]+\frac{D_{\bar{T}}}{\bar{T}_0}\left[\left(\frac{\partial T}{\partial r}\right)^2+\left(\frac{\partial T}{\partial z}\right)^2\right]\right\} \tag{5}$$

$$\left[v\frac{\partial C}{\partial r}+u\frac{\partial C}{\partial z}\right]=D_B\left[\frac{\partial^2 C}{\partial r^2}+\frac{1}{r}\frac{\partial C}{\partial r}+\frac{\partial^2 C}{\partial z^2}\right]+\frac{D_{\bar{T}}}{T_0}\left[\frac{\partial^2 T}{\partial r^2}+\frac{1}{r}\frac{\partial T}{\partial r}+\frac{\partial^2 T}{\partial z^2}\right], \tag{6}$$

where $\tau=\frac{(\rho C)_P}{(\rho C)_f}$ is the ratio between the effective heat capacity of the nanoparticle material and heat capacity of the fluid, p is pressure, C is the nanoparticle phenomena. The ambient values of T and C are denoted by T_0 and C_0 when r tend to h, D_B is the Brownian diffusion coefficient and D_T is the thermospheric diffusion coefficient.

The boundary conditions for temperature and concentration are

$$\frac{\partial T}{\partial r}=0,\frac{\partial C}{\partial r}=0 \text{ at } r=0 \tag{7}$$

$$T=T_0, C=C_0 \text{ at } r=h(z). \tag{8}$$

Introducing the following non-dimensional quantities

$$\bar{z}=\frac{z}{L},\bar{\delta}=\frac{\delta}{R_0},\bar{R}=\frac{R}{R_0},\bar{P}=\frac{P}{\frac{\mu UL}{R_0^2}},\bar{u}=\frac{u}{U},\bar{v}=\frac{L}{U\delta}v,$$

$$Re=\frac{\rho R_0 U}{\mu},\ \theta_t=\frac{T-T_0}{T_0},\sigma=\frac{C-C_0}{C_0},N_b=\frac{(\rho C)_P D_B C_0}{(\rho C)_f\,\alpha_1},$$

$$N_t=\frac{(\rho C)_P D_T T_0}{(\rho C)_f \alpha_1},\qquad G_r=\frac{\rho g\alpha_1 T_0 R_0^3}{\mu},\qquad B_r=\frac{\rho g\alpha_1 C_0 R_0^3}{\mu} \tag{9}$$

By substituting the non-dimensional variables in Eqs. (2) to (6) with the mild stenosis approximations $\frac{\delta}{R_0}\ll 1$, $R_e\,(2\delta/L_0)<<1$ and $2R_0/L_0 \sim O(1)$, the equations are reduced to (after dropping the bars)

$$\frac{\partial v}{\partial r}+\frac{v}{r}+\frac{\partial u}{\partial z}=0$$

(10)

$$\frac{\partial P}{\partial r}=-\frac{\cos\alpha}{F}$$

(11)

$$\frac{\partial P}{\partial z}-\frac{\sin\alpha}{F}=\frac{1}{r}\frac{\partial}{\partial r}\left(r\frac{\partial u}{\partial r}\right)+G_r\theta_t+B_r\sigma,$$

(12)

$$\frac{1}{r}\frac{\partial}{\partial r}\left(r\frac{\partial\theta_t}{\partial r}\right)+N_b\frac{\partial\sigma}{\partial r}\frac{\partial\theta_t}{\partial r}+N_t\left(\frac{\partial\theta_t}{\partial r}\right)^2=0$$

(13)

$$\frac{1}{r}\frac{\partial}{\partial r}\left(r\frac{\partial\sigma}{\partial r}\right)+\frac{N_t}{N_b}\left(\frac{1}{r}\frac{\partial}{\partial r}\left(r\frac{\partial\theta_t}{\partial r}\right)\right)=0$$

(14)

where U is the velocity averaged over section of the tube with radius R_0, $\theta_t, \sigma, N_b, N_t, G_r$ and B_r are temperature profile, nanoparticle phenomena, Brownian motion parameter,thermophoresis parameter, local temperature Grashof number and local nanoparticle Grashof number.

The non-dimensional boundary conditions are

$$\frac{\partial u}{\partial r}=0, \qquad at\ r=0,$$

$$u=u_B, \frac{\partial u}{\partial r}=\frac{\beta}{\sqrt{D_a}}(u_B-u_p)\ at\ r=h(z)$$

Where r and z are the coordinates and z is taken as the centre line of the tube and r transverse to it, u_B is slip velocity, u and v are the velocity components in the r and z directions respectively. β is the slip parameter and D_a is Darcy number.

The non dimensional boundary conditions for θ_t and σ are

$$\frac{\partial\theta_t}{\partial r}=0, \frac{\partial\sigma}{\partial r}=0 \ \ at\ r=0$$

$$\theta_t=0, \qquad \sigma=0 \ \ at\ r=h(z).$$

SOLUTION

Homotopy perturbation method is used to solve the equations (13) and (14) The homotopy for the equations (13) and (14) are as follows

$$H(q_t,\theta_t) = (1-q_t)[L(\theta_t) - L(\theta_{t0})] + q_t\left[L(\theta_t) + N_b\frac{\partial\sigma}{\partial r}\frac{\partial\theta_t}{\partial r} + N_t\left(\frac{\partial\theta_t}{\partial r}\right)^2\right]$$

(15)

$$H(q_t,\sigma) = (1-q_t)[L(\sigma) - L(\sigma_0)] + q_t\left[L(\sigma) + \frac{N_t}{N_b}\left(\frac{1}{r}\frac{\partial}{\partial r}\left(r\frac{\partial\theta_t}{\partial r}\right)\right)\right]$$

(16)

where q_t is the embedding parameter $(0 \le q_t \le 1)$, $L = \frac{1}{r}\frac{\partial}{\partial r}\left(r\frac{\partial}{\partial r}\right)$ is the linear operator, and the initial guesses θ_0 and σ_0 are

$$\theta_0(r,z) = \left(\frac{r^2-h^2}{4}\right), \qquad \sigma_0(r,z) = -\left(\frac{r^2-h^2}{4}\right)$$

(17)

Define

$$\theta_t(r,z) = \theta_0 + q_t\theta_1 + q_t^2\theta_2 + \cdots$$

(18)

$$\sigma(r,z) = \sigma_0 + q_t\sigma_1 + q_t^2\sigma_2 + \cdots$$

(19)

The above two series are convergent in most of the cases. The rate of convergence depends on the nonlinear part of the equation.

Therefore, the solution for temperature and concentration are obtained for $q_t = 1$ as

$$\theta_t(r,z) = \left(\frac{r^4-h^4}{64}\right)(N_b - N_t)$$

(20)

$$\sigma(r,z) = -\left(\frac{r^2-h^2}{4}\right)\frac{N_t}{N_b}.$$

(21)

Substituting the equat (20) and (21) in equation (12) and solving it for the velocity, we get

$$u(r,z) = \left(\frac{\sqrt{D_a}}{2\beta}h + \frac{r^2-h^2}{4} - D_a\right)\frac{dP}{dz} + \frac{G_r(N_b-N_t)}{64}\left(\frac{h^5r^6\sqrt{D_a}}{108\beta} + \frac{r^2h^2}{4} - \frac{2h^6}{9}\right) + B_r\frac{N_t}{N_b}\left(\frac{r^4}{64} - \frac{r^2h^2}{16} + \frac{3h^4}{64} - \frac{\sqrt{D_a}\,h^3}{4\beta}\right) - \frac{\sin\alpha}{F}\left(\frac{\sqrt{D_a}}{2\beta}h + \frac{r^2-h^2}{4}\right)$$

(22)

The flow rate Q is given by

$$Q = \int_0^h 2ru\,dr.$$

(23)

$$Q=\left(\frac{\sqrt{D_a}}{2\beta}h^3-\frac{h^4}{8}-D_a h^2\right)\frac{dP}{dz}+\frac{G_r(N_b-N_t)}{32}\left(\frac{h^7\sqrt{D_a}}{6\beta}-\frac{33h^8}{288}+\frac{h^6}{16}\right)+B_r\frac{N_t}{2N_b}\left(\frac{7h^6}{96}-\frac{\sqrt{D_a}h^5}{8\beta}\right)-\frac{\sin\alpha}{F}\left(\frac{\sqrt{D_a}}{2\beta}h^3-\frac{h^4}{8}\right)$$

(24)

From equation (24), $\frac{dP}{dz}$ can be written as

$$\frac{dP}{dz}=\frac{1}{\left(\frac{\sqrt{D_a}}{2\beta}h^3-\frac{h^4}{8}-D_a h^2\right)}\left(Q-\frac{G_r(N_b-N_t)}{32}\left(\frac{h^7\sqrt{D_a}}{6\beta}-\frac{33h^8}{288}+\frac{h^6}{16}\right)-B_r\frac{N_t}{2N_b}\left(\frac{7h^6}{96}-\frac{\sqrt{D_a}h^5}{8\beta}\right)+\frac{\sin\alpha}{F}\left(\frac{\sqrt{D_a}}{2\beta}h^3-\frac{h^4}{8}\right)\right)$$

(25) The pressure drop Δp across the stenosis between the section $z=0$ and $z=l$ is obtained from eq. (25) as

$$\Delta p=-\int_0^l\frac{dp}{dz}\,dz$$

(26)

The resistance to the flow λ is given by

$$\lambda=\frac{1}{Q}\int_0^l-\frac{dp}{dz}dz$$

(27)

The pressure drop in the absence of stenosis ($h=1$) is denoted by Δp_N, is obtained from eq.(26) as

$$\Delta p_N=-\int_0^l\left(\frac{dp}{dz}\right)_{h=1}dz$$

(28)

The resistance to the flow in the absence of stenosis is denoted by λ_N is obtained from eq.(26), as $\lambda_N=\frac{1}{Q}\int_0^l-\left(\frac{dp}{dz}\right)_{h=1}dz$

The impedance is calculated as

$$\bar{\lambda}=\frac{\lambda}{\lambda_N}$$

(29)

The wall shear stress is calculated as

$$S_{rz} = -\frac{h}{2}\frac{dp}{dz} \qquad (\text{}$$

RESULTS AND ANALYSIS

In this part of the article, we have discussed the effects of various physical parameters on velocity (u), temperature distribution (θ_t), nanoparticle phenomena (σ), impedance (λ) and wall shear stress (τ_h).

Velocity profile

The velocity profile (u) is plotted against the radial axis (r) for different values of stenosis height (δ), Brownian motion number $([\![N]\!]_b)$, thermophoresis parameter $([\![N]\!]_t)$, and angle of inclination (α), Darcy number $(\sqrt{D_a})$, slip parameter (β), local nanoparticle Grashof number $([\![B]\!]_r)$, local temperature Grashof number $([\![G]\!]_r)$, in Figs.2-9. It is noticed that the variation in velocity is symmetrical for all the parameters. It is also observed that the velocity increases with the stenosis height, thermophoresis parameter $([\![N]\!]_t)$, inclination (α), slip parameter(β), local nanoparticle Grashof number $([\![B]\!]_r)$, local temperature Grashof number $([\![G]\!]_r)$ and the flow velocity is more at the center of the tube and minimum at the stenosis walls.

But the velocity decreases with the Brownian parameter $([\![N]\!]_b)$ and Darcy number $(\sqrt{D_a})$, i.e. the velocity is minimum at the centre and maximum at the walls.

Temperature Profile

Form Figs. 10-11, it is noticed that the temperature distribution decreases with the increase of the Brownian motion number $([\![N]\!]_b)$, and increases with thermophoresis parameter $([\![N]\!]_t)$. The temperature is minimum in the region $-0.5 \leq r \leq 0.5$.

Nano-particle phenomenon

Figs. 12-13, shows the variation of nanoparticle phenomena (σ) for the Brownian motion parameter $([\![N]\!]_b)$ and thermophoresis parameter $([\![N]\!]_t)$. It is observed that the nanoparticle phenomena increases with the increase of thermophoresis parameter $([\![N]\!]_t)$ but it decreases with Brownian motion number $([\![N]\!]_b)$ and it is miximum at the center of the tube (i.e $r = 0$) and minimum at the walls.

Impedance variation

In Figs.14-19, the impedance is plotted against to the stenosis height for various values of Brownian motion number (N_b), thermophoresis parameter (N_t), local nanoparticle Grashof number (B_r), local temperature Grashof number (G_r), slip parameter (β), Darcy number $(\sqrt{D_a})$.

It is seen that, the impedance increases with stenosis height (δ) and local temperature Grashof number (G_r) but decreases with thermophoresis parameter (N_t), Brownian motion number (N_b), local nanoparticle Grashof number (B_r), Darcy number $(\sqrt{D_a})$ and slip parameter (β).

The variation in impedance against to the Darcy number for various values of thermophoresis parameter (N_t), Brownian motion number (N_b) is shown in Figs. 20-21. It is noticed that the impedance of the flow decreases with Darcy number $(\sqrt{D_a})$ and Brownian motion parameter (N_b) while it increases with thermophoresis parameter (N_t).

Shear stress profile

The variation of shear stress against the axial direction z for different values of stenosis height (δ), angle of inclinatiion (α), slip parameter (β), Darcy number $(\sqrt{D_a})$.

Brownian motion number (N_b), thermophoresis parameter (N_t), local temperature Grashof number (G_r), local nanoparticle Grashof number (B_r), and inclinatiion (α) are shown in Figs. 22-25.

From Fig 22, it is observed that the shear stress is directly proportional to the height of the stenosis i.e the shear stress increases with the stenosis height attains maximum at $z = 0.26, z = 0.53$ and minimum at $(z = 0.4)$. It is also observed that the shear stress increases with angle of inclination (α) and slip parameter (β) while it decreases with Darcy number $(\sqrt{D_a})$ (Figs. 23-24).

Streamline patterns

The streamline patterns for different parameters like height of stenosis (δ), Darcy number $(\sqrt{D_a})$ and inclination (α) are represented in Figs.26-28. The number of boluses increase and size is expanded as the stenosis height (δ) increases (Fig.26). The effect of Darcy number and inclination are carried out in figs 27-28. It is found that the number of boluses decrease with the increase of Darcy number and inclination.

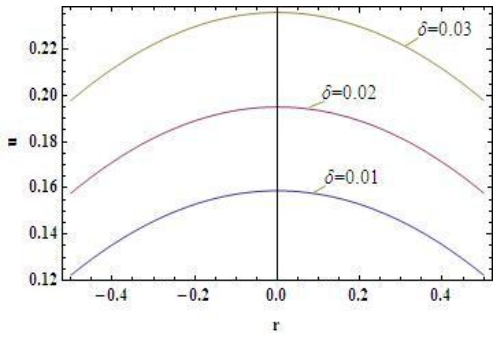

Figure 2: Variation in velocity for δ

$(d = 0.2, L_0 = 0.4, Q = 0.1, L = 1, F = 0.8)$

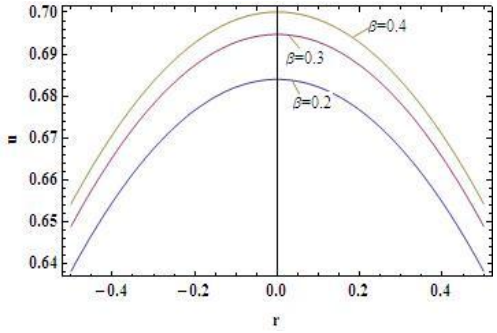

Figure 3: Variation in velocity for β

$(d = 0.2, L_0 = 0.4, Q = 0.1, L = 1, F = 0.8)$

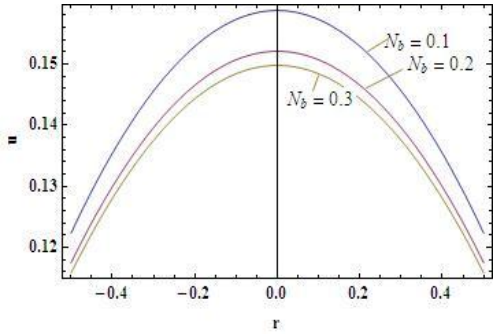

Figure 4: Variation in velocity for N_b

$(d = 0.2, L_0 = 0.4, Q = 0.1, L = 1, F = 0.8)$

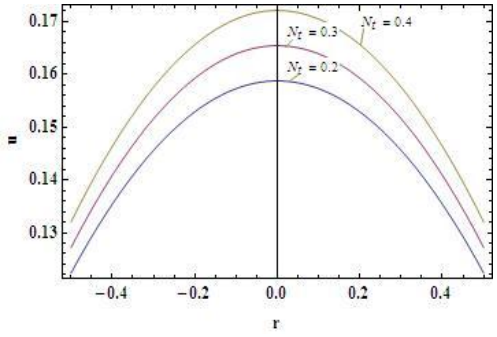

Figure 5: Variation in velocity for N_t

$(d = 0.2, L_0 = 0.4, Q = 0.1, L = 1, F = 0.8)$

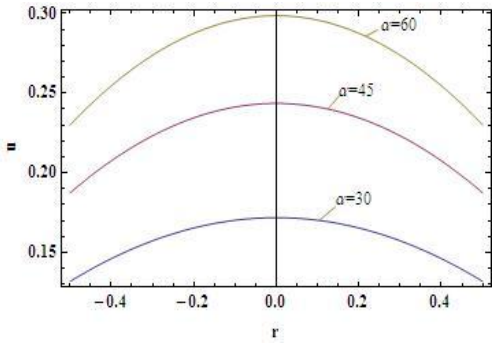

Figure 6: Variation in velocity for α

$(d = 0.2, L_0 = 0.4, Q = 0.1, L = 1, F = 0.8)$

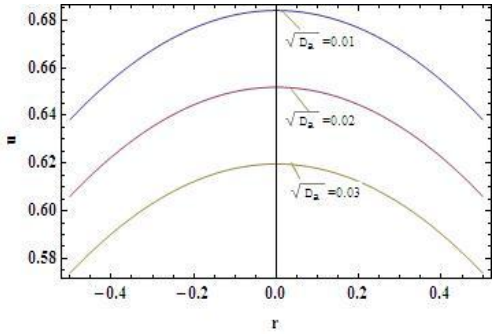

Figure 7: Variation in velocity for $\sqrt{D_a}$

$(d = 0.2, L_0 = 0.4, Q = 0.1, L = 1, F = 0.8)$

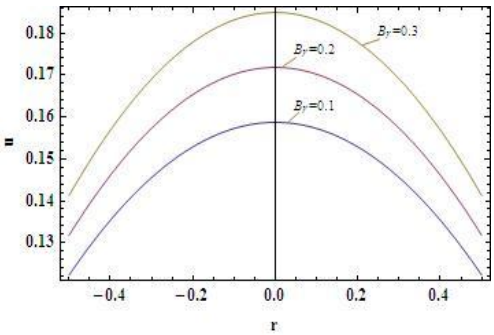

Figure 8: Variation in velocity for B_r

$(d = 0.2, L_0 = 0.4, Q = 0.1, L = 1, F = 0.8)$

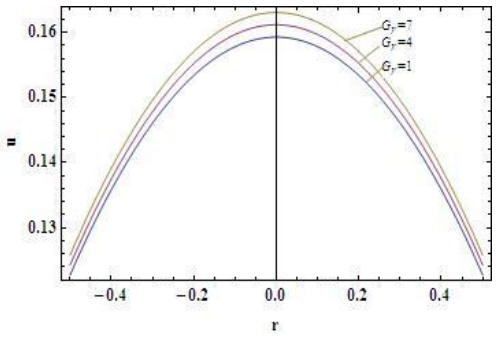

Figure 9: Variation in velocity for G_r

$(d = 0.2, L_0 = 0.4, Q = 0.1, L = 1, F = 0$

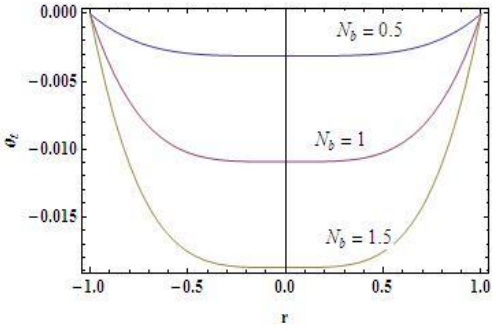

Figure 10:Variation in Temperature for

$N_b(d = 0.2, L_0 = 0.4, L = 1, \delta = 0.02)$

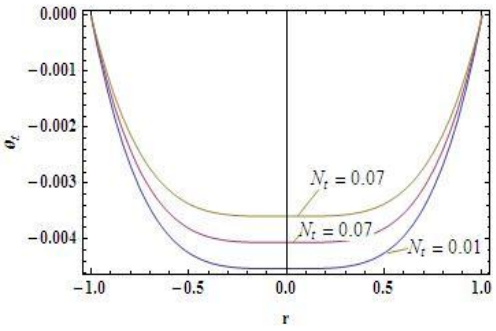

Figure 11:Variation in Temperature for N_t

$(d = 0.2, L_0 = 0.4, L = 1, \delta = 0.02)$

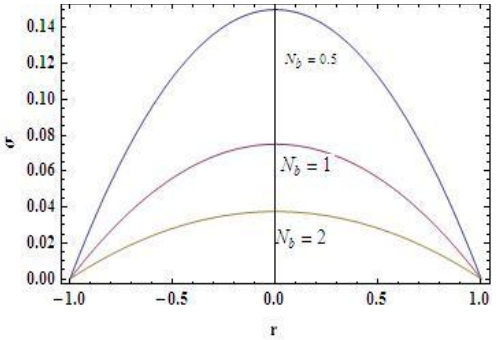

Figure 12: Concentration profile for N_b

$(d = 0.2, L_0 = 0.4, L = 1, \delta = 0.02)$

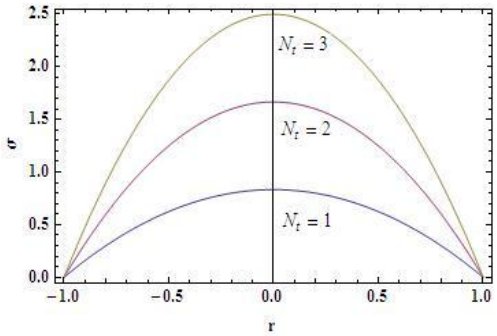

Figure 13: Concentration profile for N_t

$(d = 0.2, L_0 = 0.4, L = 1, \delta = 0.02)$

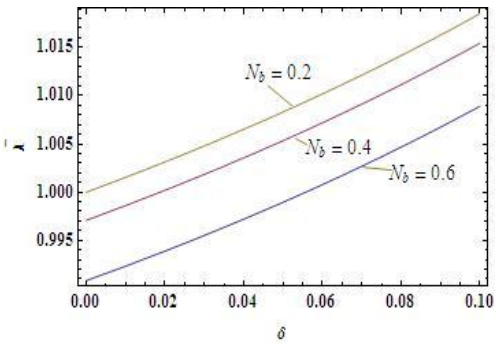

Figure-14: Variation in impedance for N_b

$(d = 0.2, L_1 0 = 0.4, Q = 1.01, L = 1 \ \ F = 0.8,$

$G_1 r = 1, \alpha = \pi/6, B_1 r = 0.3, \beta = 0.02, \sqrt{(D_1 a)} = 1)$

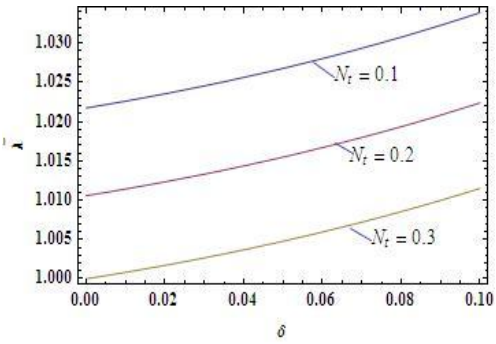

Figure-15: Variation in impedance for N_t

$(d = 0.2, L_1 0 = 0.4, Q = 1.01, L = 1, F = 0.8,$

$G_1 r = 1, \alpha = \pi/6, \beta = 0.02\sqrt{(D_1 a)} = 1)$

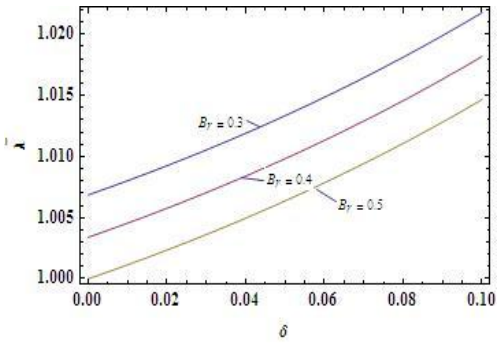

Figure-16: Variation in impedance for B_r

$(d = 0.2, L_\downarrow 0 = 0.4, Q = 1.01, L = 1, F = 0.8,$

$G_\downarrow r = 1, \alpha = \pi/6, \beta = 0.02 \sqrt{(D_\downarrow a)} = 1)$

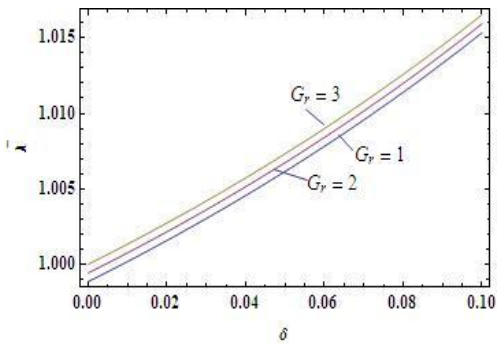

Figure-17: Variation in impedance for G_r

$(d = 0.2, L_\downarrow 0 = 0.4, Q = 1.01, L = 1, F = 0.$

$G_\downarrow r = 1, \alpha = \pi/6, \beta = 0.02 \sqrt{(D_\downarrow a)} = 1)$

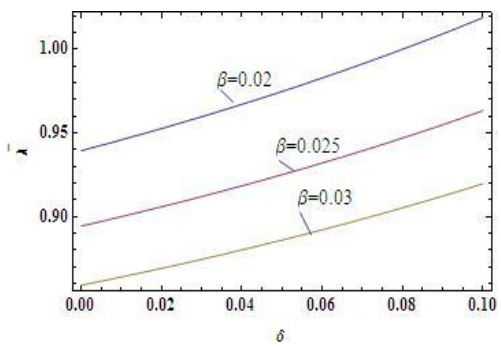

Figure-18: Variation in impedance for β

$(d = 0.2, L_\downarrow 0 = 0.4, Q = 1.01, L = 1,$

$F = 0.8, G_\downarrow r = 1, \alpha = \pi/6, B_\downarrow r = 0.3, , \sqrt{(D_\downarrow a)} = 1)$

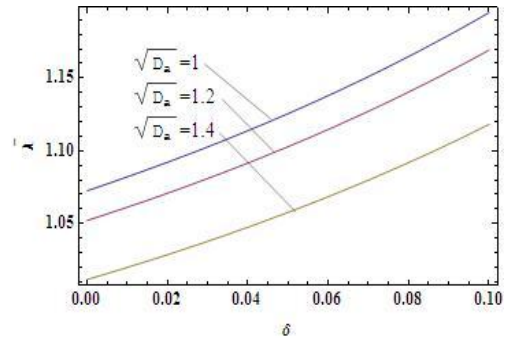

Figure-19: Variation in impedance for $\sqrt{D_a}$

$(d = 0.2, L_\downarrow 0 = 0.4, Q = 1.01, L = 1$

$F = 0.8, G_\downarrow r = 1, \alpha = \pi/6, B_\downarrow r = 0.3, \beta = 0.02,)$

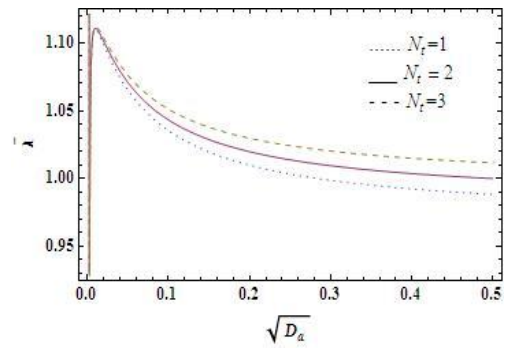

Figure-20: Variation in impedance for N_t

$(d = 0.2, L_\downarrow 0 = 0.4, Q = 1.01, L = 1, F = 0.8,$

$N_\downarrow b = 0.1, \alpha = \pi/6, B_\downarrow r = 0.3, \beta = 0.02, \sqrt{(D_\downarrow a)} = 1)$

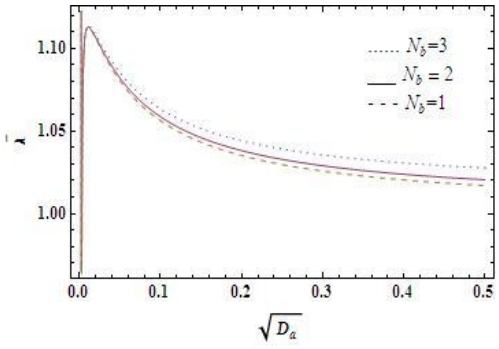

Figure-21: Variation in impedance for N_b

$(d = 0.2, L_\downarrow 0 = 0.4, Q = 1.01, L = 1, F = 0.8, N_\downarrow t = 0.2,$

$\alpha = \pi/6, B_\downarrow r = 0.3, \beta = 0.02, \sqrt{(D_\downarrow a)} = 1)$

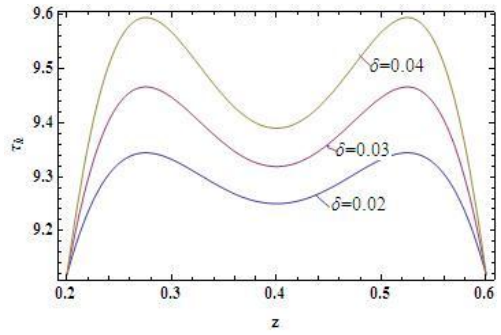

Figure-22: Wall shear stress variation for δ

$(d = 0.2, L_1 0 = 0.4, Q = 1.01, L = 1, F = 0.$

$[N_1 b = 0.1, N]_1 t = 0.2, \alpha = \pi/6, B_1 r = 0.3, \beta = 0.02, \sqrt{(D_1 a)} =$

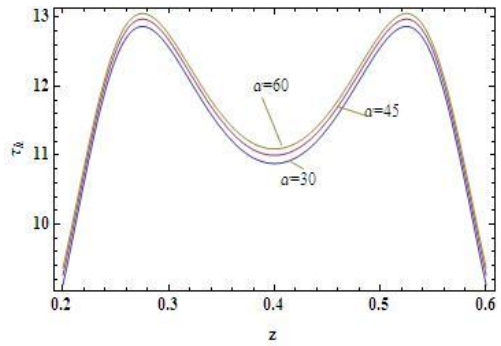

Figure-23: Wall shear stress variation for α

$\left(d = 0.2, L_0 = 0.4, Q = 1.01, L = 1, F = 0.8, N_b = 0.1, N_t = 0.2, B_r = 0.3, \beta = 0.02, \sqrt{D_a} =\right.$

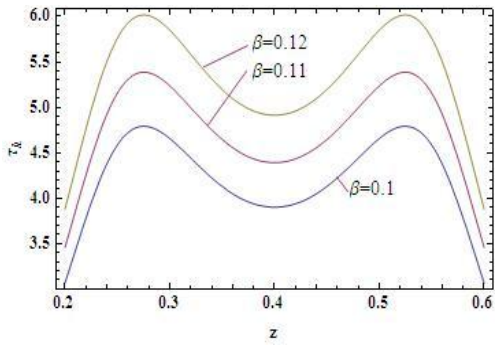

Figure-24: Wall shear stress variation for β

$(d = 0.2, L_1 0 = 0.4, Q = 1.01, L = 1, F = 0.$

$[N_1 b = 0.1, N]_1 t = 0.2, \alpha = \pi/6, B_1 r = 0.3, \sqrt{(D_1 a)}$

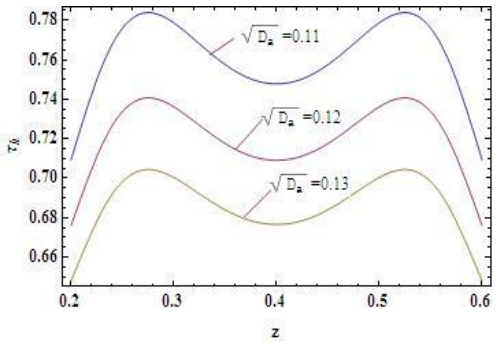

Figure-25: Wall shear stress variation fo $r \sqrt{D_a}$

$(d = 0.2, L_1 0 = 0.4, Q = 1.01, L = 1, F = 0.8,$

$[N_1 b = 0.1, N]_1 t = 0.2, \alpha = \pi/6, B_1 r = 0.3, \beta = 0.02,)$

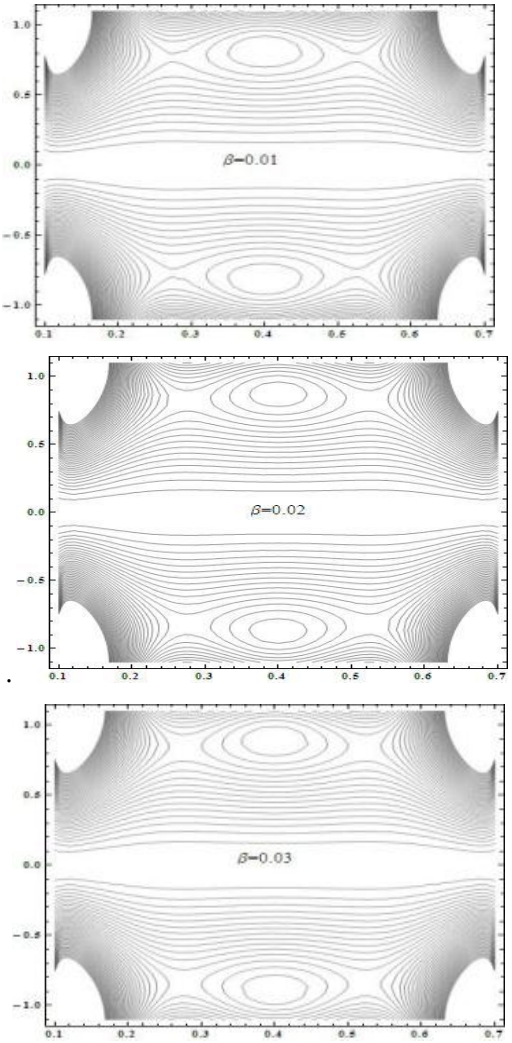

Figure-26: Stream lines for different values of β

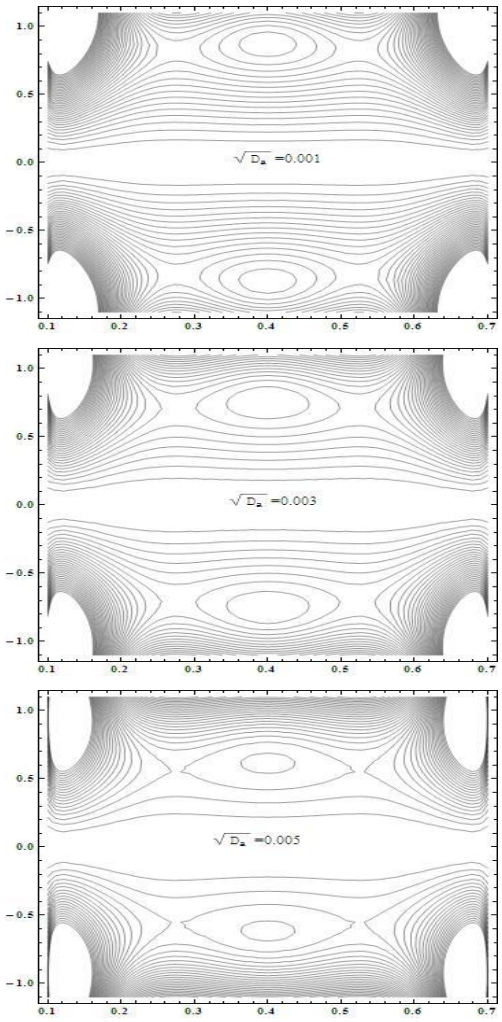

Figure-27: Stream lines for different values of $\sqrt{D_a}$

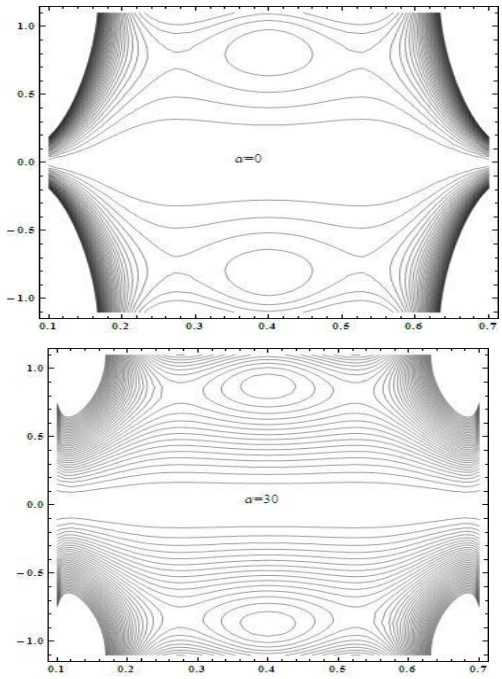

Figure 28: Stream lines for different values of α

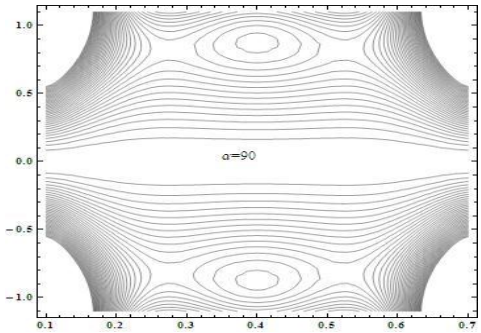

CONCLUSIONS

The present study examines the steady flow of Nanofluid in an inclined tube with an overlapping stenosis and permeable walls. HPM method is used to get the exact solutions for temperature distribution, nanoparticle phenomena, pressure drop, flow resistance and wall shear stress.

The key points of the performed analysis are as follows:

- The velocity increases with the increase in stenosis height, thermophoresis parameter $(N]_t)$, inclination (α), slip parameter(β), local nanoparticle Grashof number $(B]_r)$, local temperature Grashof number $(G]_r)$. While it decreases with the Brownian parameter $(N]_b)$ and Darcy number $(\sqrt{D_a})$.
- The temperature distribution decreases with the increase of the Brownian motion number $(N]_b)$, and increases with thermophoresis parameter $(N]_t)$.
- The impedance of the flow decreases with Darcy number $(\sqrt{D_a})$ and Brownian motion parameter $(N]_b)$ while it increases with thermophoresis parameter $(N]_t)$.
- The shear stress increases with angle of inclination (α) and slip parameter (β) while it decreases with Darcy number $(\sqrt{D_a})$.
- The number of boluses decrease with the increase of Darcy number and inclination.

REFERENCES

1. Deplano V, Bertolottic C, Boiron O. Numerical simulations of unsteady flows in a stenosed coronary bypass graft. Med Biol Eng Comput. 2001; 39:488-499.
2. Sankar DS. Two phase non-linear model for blood flow in asymmetric and axi-symmetric stenosed arteries. Int J Non Linear Mech. 2011; 46:296-305.
3. Srivastava LM. Flow of couple stress fluid through stenotic blood vessels. J Biomech. 1985; 18:479-485.
4. Srivastava N. Analysis of flow characteristics of the blood flowing through an inclined tapered porous artery with mild stenosis under the influence of an inclined magnetic field. J. Bio Phys. 2014; 9: 797142.
5. Srivastava VP. Arterial blood flow through a non-symmetric stenosis with applications, Japanese J. Appl. Phys. 1995; 34: 6539-6545.
6. Mustapha N, Amin N, Chakravarthy S, Mandal PK. Unsteady magnetohydrodynamic blood flow through irregular multi-stenosed arteries, Coput. Biol Med. 2009; 39: 896-906.
7. Ismail Z, Abdullah I, Mustapha N and Amin N. A power law model of blood flow through a tapered overlapping stenosed artery, Appl Mathematics and Comput. 2008; 195: 669-680.
8. Mekheimer Kh, El Kot MA. Mathematical modeling of unsteady flow of a Sisko fluid through an anosotropically tapered elastic arteries with time variant overlapping stenosis, Appl Math. Model. 2012; 36: 5393-5407.
9. Riahi DN, Roy R, Cavazos S. on arterial blood flow in the presence of an overlapping stenosis, Math Comput Model. 2011; 54: 2999-3006.

10. Choi SUS. Enhancing thermal conductivity of fluids with nanoparticles, In: Signer DA, Wang HP (eds) Developments and applications of Non-Newtonian Flows, ASME, New York, 1995; 66: 99-105.
11. Nadeem S, Ijaz S and Akbar NS. Nanoparticle analysis for blood flow of Prandtl fluid model with stenosis, Int Nano Letters. 2013; 3: 1-13.
12. Eldable NTM, Abo-Seida OM , Abo-Seliem AS, Elshekhipy AA and Nda Hegazy. Peristaltic transport of magnetohydrodynamic Carreau Nanofluid with heat and mass transfer inside asymmetric channel 7: 1-20.
13. Akbar NS and Adil Wahid Butt, Entropy generation analysis in convective Ferromagnetic Nano blood flow through a composite stenosed arteries with permeable walls, Commun. Theor. Phys. 2017; 67: 554-560.
14. Akbar NS, Rahman SU, Ellahi R, Nadeem S, Nano fluid fow in tapering stenosed arteries with permeable walls, Int J Thermal Sciences. 2014; 85: 54-61.
15. Akbar NS and Adil Wahid Butt, Magnetic field effects for copper suspended nanofluid venture through a composite stenosed arteries with permeable walls. Journal of Magnetism and magnetic materials. 2015; 381: 285-291.
16. Ellahi R, Rahman SU, Nadeem S and Akbar NS, Blood flow of nanofluid through an artery with composite stenosis and permeable walls, Appl. Nanosci. 2014; 4: 919-926.
17. Maruthi Prasad K, Sudha T and Mahabaleshwar U.S, Flow of nanofluid through an inclined tube of non uniform cross section with multiple stenoses, Int. J. Energy and Thermal Fluid. 2017; 1(1): 14-31.